Hyperhomocysteinemia-Induced Alterations in Protein Expression and Oxidative Stress Parameters in Rat Heart

Zuzana TATARKOVÁ[1#], Lucia LICHARDUSOVÁ[2#], Terézia LYSIKOVÁ[1], Monika KMEŤOVÁ SIVOŇOVÁ[1], Peter RAČAY[1], Ján LEHOTSKÝ[1], Peter KAPLÁN[1]

[#]*These authors contributed equally to this work*

[1]Department of Medical Biochemistry, Comenius University in Bratislava, Jessenius Faculty of Medicine, Martin, Slovakia, [2]Biomedical Centre Martin, Comenius University in Bratislava, Jessenius Faculty of Medicine, Martin, Slovakia

Received November 8, 2023
Accepted March 13, 2024

Summary

Hyperhomocysteinemia (HHcy) is considered an independent risk factor of cardiovascular diseases. Among the proposed mechanisms underlying homocysteine toxicity are altered protein expression and induction of oxidative stress. In the present study, we explored protein abundance and parameters related to oxidative stress in heart homogenates of rats exposed to chronic mild HHcy. Using two-dimensional gel electrophoresis followed by MALDI-TOF/TOF mass spectrometry 22 altered proteins (6 upregulated and 14 downregulated) were identified. For eight proteins the altered abundances were validated by Western blot analysis. Identified proteins are primarily involved in energy metabolism (mainly enzymes of glycolysis, pyruvate dehydrogenase complex, citric acid cycle, and ATP synthase), cardiac muscle contraction (α-actin and myosin light chains), stress response (heat-shock protein β1 and αB-crystallin) and antioxidant defense (glutathione peroxidase 1). Diminished antioxidant defense was confirmed by decreases in total antioxidant capacity and GSH/GSSG ratio. Consistent with the decline in enzymatic and non-enzymatic antioxidant defense the protein oxidative modification, as determined by tyrosine nitration, was significantly increased. These findings suggest that both, altered protein expression and elevated oxidative stress contribute to cardiovascular injury caused by HHcy.

Keywords: Homocysteine • Heart • Protein abundance • Antioxidant capacity • Nitrotyrosines

Corresponding author

Peter Kaplan, Department of Medical Biochemistry, Comenius University in Bratislava, Jessenius Faculty of Medicine, Mala Hora 4D, 036 01 Martin, Slovakia. Email: peter.kaplan@uniba.sk

Introduction

Cardiovascular diseases (CVDs) are a leading cause of morbidity and mortality worldwide. In addition to classic risk factors, such as hypertension, hypercholesterolemia, obesity, and smoking, hyperhomocysteinemia (HHcy) has been recognized as a new independent risk factor [1]. Homocysteine (Hcy) is a non-protein amino acid formed during the metabolism of the essential amino acid methionine. HHcy can be caused by several diseases, drug treatment, or deficiencies in enzymes and vitamins which are required as cofactors in the metabolic pathway. HHcy is categorized as mild (15-30 μM), intermediate (31-100 μM), and severe (>100 μM). While severe HHcy is rare, mild HHcy or intermediate HHcy are quite common in the general population and are involved in a variety of CVDs, including coronary artery disease, peripheral arterial disease, venous thrombosis, myocardial infarction, and heart failure.

Although the molecular mechanisms that lead to cardiovascular injury at HHcy are still not completely understood, several *in vitro* and *in vivo* studies have indicated that dysregulations in gene expression contribute to this phenomenon [2]. For example, numerous genes, including those involved in cell metabolism and immune response, were differentially

expressed in the hearts of dogs with chronic mild HHcy [3]. Experimental evidence also indicates that HHcy alters the expression of several mitochondrial proteins [4-6]. An alternative mechanism that might be involved in Hcy toxicity is increased oxidative stress and attenuated NO bioavailability [3,7-12]. Both proposed mechanisms of HHcy-induced injury, altered gene expression, and oxidative stress are not mutually exclusive, because several studies have proposed oxidative stress as a result of decreased expression of antioxidant enzymes and redox balance regulating proteins [3,9]. Overproduction of superoxide radicals and NO leads to their spontaneous combination to form peroxynitrite ($ONOO^-$), a powerful oxidant that can directly attack proteins to cause tyrosine nitration [13]. Elevated nitration of cardiac proteins was observed in various conditions, including cardiac aging [14], ischemia-reperfusion [15], and HHcy [16,17]. Although oxidative stress seems to be the well-established mechanism of HHcy-induced injury, actually several studies fail to show increased production of ROS/RNS or accumulation of oxidative damage in the heart at HHcy. For example, studies on isolated cardiac mitochondria have shown that HHcy decreased ROS production [18]. Similarly, the production of ROS and markers of lipid peroxidation (LPO) were not elevated in isolated rat hearts perfused with Hcy [10]. Our studies have shown that mild chronic HHcy alters expressions and functions of proteins in rat cardiac mitochondria and sarcoplasmic reticulum, but there was no evidence of their oxidative damage [6,19]. Nevertheless, our study has suggested that oxidative stress occurred in the heart since lipid peroxidation in homogenates was significantly increased as compared to control [6].

The aim of the present study is to complement the previously demonstrated effects of HHcy on cardiac mitochondria and sarcoplasmic reticulum with investigations on protein expression and oxidative stress in the whole heart homogenates of hyperhomocysteinic rats. Our results support the view that both altered protein expression and elevated oxidative stress are involved in the mechanism of adverse effects of HHcy on the heart.

Methods

Animals

The study was performed on 4-month-old male Wistar rats (weighing 300-400g) supplied by the Institute of Experimental Pharmacology, Slovak Academy of Sciences, Dobra Voda, Slovakia. They were acclimatized for 1 week in a controlled environment with a 12 h light/dark cycle and an ambient temperature of 22±2 °C and with food and water *ad libitum*. After acclimatization rats were randomly divided into two groups: control (n=5) and hyperhomocysteinemic (n=5). Treatment with Hcy and determination of plasma Hcy level were performed as described previously [6], DL-homocysteine (0.45 μmol/g of body weight) was injected subcutaneously, twice a day (with 8-hour intervals) for 2 weeks. Control group was treated with saline solution in the same manner as the HHcy group. After this treatment, rats were sacrificed by decapitation under anesthesia with halothane. The hearts were rapidly removed and placed into ice-cold Krebs-Henseleit solution and cannulated through the aorta for perfusion according to the Langendorff method as described previously [19]. At the end of perfusion, hearts were frozen and stored at -80 °C for the preparation of homogenates. All procedures involving animals were performed following the European Community guidelines and were approved by the Ethical Committee of the Jessenius Faculty of Medicine.

Preparation of tissue homogenates

Tissue homogenates were prepared from frozen hearts essentially as described previously [19]. Frozen tissue of the whole heart was thawed in 10 volumes of ice-cold homogenization buffer (pH 7.0) containing 30 mM KH_2PO_4, 5 mM EDTA, 0.3 M sucrose, 0.3 mM phenylmethylsulfonyl fluoride and homogenized 5 times for 25 s with a Teflon pestle in Potter-Elvehjem homogenizer. Protein concentration was determined with the DC Protein assay kit (500-0111, Bio-Rad Laboratories) using the BioTek Synergy H4 hybrid microplate reader (Agilent Technologies).

Two-dimensional (2D) gel electrophoresis

Heart homogenates (250 μg of protein) were precipitated 2 times with ice-cold acetone and centrifuged at 16 200 g for 10 min. Protein pellet was resuspended with a rehydration solution containing 8M urea, 2 % CHAPS, 50mM DTT, 0.2 % Bio-Lyte 3/10 ampholyte, and 0.001 % bromphenol blue. The first-dimension was performed on ReadyStrip IPG strips pH 3-10 (Bio-Rad Laboratories) using the Protean IEF system (Bio-Rad Laboratories) as follows: 250 V for 20 min, 8 000 V for 2 h and then until the total voltage reached 10 000 Vh. After isoelectric focusing, the strips were

equilibrated for 15 min in 375mM Tris-HCl, pH 8.8, 6M urea, 2 % SDS, and 2 % DTT) followed by 15 min equilibration in the same buffer, except that 0.03g/ml iodoacetamide was added instead of DTT. The second dimension was performed on 12 % polyacrylamide gels at an electric current of 15 mA for 20 min and then at 25 mA until the bromophenol blue dye reached the gel bottom. Staining of gels was performed with Bio-Safe Coomassie G-250 stain (Bio-Rad Laboratories). Stained gels were scanned by GS-800 Calibrated Densitometer (Bio-Rad Laboratories) and analyzed using PDQuest 8 software (Bio-Rad Laboratories). Spots showing differential abundance greater than 2.0 ($p<0.05$) or lower than 0.5 ($p<0.05$) were used for further analysis.

In-gel digestion and preparation of samples for MS analysis

Differentially abundant protein spots were manually excised from the gels and destained with 50 % acetonitrile (CH_3CN) in 25 mM ammonium bicarbonate at room temperature (RT) overnight and washed in 100 % CH_3CN for 15 min. After drying, the gel pieces were reduced with 100 µl of 10mM dithiothreitol (DTT) in 25 mM ammonium bicarbonate at 56 °C for 45 min and alkylated in 100 µl of 55mM iodoacetamide and 25 mM ammonium bicarbonate for 30 min in dark. Gel pieces were then rinsed in 25 mM ammonium bicarbonate and 100 % CH_3CN and dried in a SpeedVac centrifuge. The proteins were digested with trypsin for 30 min on ice, then ammonium bicarbonate was added and the digestion continued at 37°C overnight. Finally, the protein tryptic digests were dissolved in 1 µl of 10 % trifluoroacetic acid.

Identification of proteins by mass spectrometry

Protein digests were concentrated in a SpeedVac centrifuge and 0.75 µl was applied onto the AnchorChip™ target plate (Bruker Daltonics, Bremen, Germany) together with 1 µl of matrix (α-cyano-4 hydroxycinnamic acid) and allowed to dry at RT. The mass spectra of protein digests were recorded by an Ultraflex III MALDI-TOF mass spectrometer (Bruker Daltonics, Bremen, Germany) operating in a positive ion reflectron mode, with an accelerating voltage of 20 kV and pulsed extraction. The mass spectra were externally calibrated using peptide calibration standards (Bruker Daltonics). Mass spectra were collected in the mass range 700-3000 m/z by accumulation data from 2000 laser shots and were processed with FlexAnalysis software (Bruker Daltonics). Proteins were identified by a combination of peptide mass fingerprinting (PMF) and MS/MS fragmentation. MS/MS spectra were acquired for the two strongest peaks selected in each peptide mass map.

The MS and MS/MS data were combined by BioTools software (Bruker Daltonics) and were searched against the Swiss-Prot or NCBI databases using the MASCOT database search engine (Matrix Science, London, UK). The Mascot search parameters were as follows, taxonomy: rodents, one missed cleavage site allowed, carbamidomethylation as the fixed modification, methionine oxidation as the variable modification, maximum allowed error of mass 50 ppm for the MS mode and tolerance of 0.5 Da for MS/MS mode. Presented scores are combinations of MS and MS/MS measurements. Only hits with Mascot scores greater than 65 were accepted.

Western blot analysis

Proteins (40 µg) were separated by SDS-PAGE on 10 % resolving gels using a Mini-Protean electrophoresis cell (BioRad Laboratories) and transferred into Immobilon-P transfer membranes (Millipore) using Mini Trans-Blot cell (BioRad Laboratories). After blocking and rinsing, membranes were probed for 1 h with one of the following antibodies (all obtained from Santa Cruz Biotechnology, USA and diluted 1:5000): α-enolase mouse monoclonal antibody (catalog # sc/100812), β-enolase mouse monoclonal antibody (sc-100811), myoglobin mouse monoclonal antibody (sc-74525), isocitrate dehydrogenase 1/2 mouse monoclonal antibody (sc-373816), cytosolic malate dehydrogenase mouse monoclonal antibody (sc-166879), triosephosphate isomerase mouse monoclonal antibody (sc-166785), creatine kinase M/B mouse monoclonal antibody (sc-70881), mitochondrial ATP-α synthase goat polyclonal antibody (sc-49162). β-actin goat polyclonal antibody (sc-1616) was used to confirm equal loading and to normalize the measurements. After washing the primary antibody, the membranes were incubated 1 h with horseradish peroxidase-conjugated goat anti-mouse secondary antibody. The protein bands were visualized by enhanced chemiluminescence reagent, digitalized by an image analyzer (BioRad Laboratories), and quantified using GeneTools software (SynGene, India).

Protein characterization and protein-protein interactions

Cellular locations and functions of differentially abundant proteins were explored using the UniProt database. Analysis of interactions among these proteins was performed using the STRING software (http://www.string-db.org/) [20].

Total antioxidant capacity

The total antioxidant capacity (TAC) was determined using OxiSelect™ Total Antioxidant Capacity assay kit (antibodies-online, Aachen, Germany) according to the manufacturer's instructions. This method is based on the reduction of Cu (II) to Cu (I) by antioxidants present in the sample. Cu (I) further reacts with chromogenic reagent producing colored complex with maximum absorbance at 490 nm. The reductive capacity of tissue homogenates was calculated using uric acid standard curve and results are expressed as μM of copper-reducing equivalents.

Determination of total protein nitrotyrosines

The level of total protein nitrotyrosines was determined using an ELISA kit (OxisResearch, Portland, USA) according to the manufacturer's instructions. Briefly, tissue homogenates and standards were added onto a microtiter plate and incubated for 1 h at RT. Wells were then washed and nitrotyrosine antibody was added to each well and incubated for 1 h at RT. After washing the samples were incubated with streptavidin peroxidase for 1 h at RT. Next, the samples were incubated with a freshly prepared solution of tetramethylbenzidine substrate for 30 min in the dark. Finally, a stop solution was added to terminate the reaction and the absorbance was measured at 450 nm using a Bio-Tek plate reader. The levels of protein nitrotyrosines in homogenates were quantified using a standard curve.

Glutathione assay

Total (GSH+GSSG) and oxidized (GSSG) glutathione concentrations were determined using a colorimetric Glutathione Assay kit (G-Biosciences, St. Louis, USA) according to the manufacturer's instructions. Briefly, total glutathione was determined in deproteinated tissue samples after the reduction of GSSG to GSH by glutathione reductase and reaction with 2-2`-dithiobis[2-nitrobenzoic acid] (DTNB) by measuring the absorbance at 415 nm and comparing it with a standard curve. GSSG was quantified after blocking free thiols with derivatizing reagent 4-vinylpyridine. GSH concentration was calculated by subtracting GSSG concentration from the total glutathione concentration.

Statistical analysis

Data are expressed as mean ± standard error of the mean (SEM). Two-tailed Student`s t-test was used to evaluate differences between HHcy and control groups. A value of $p<0.05$ was considered statistically significant.

Results

Hyperhomocysteinemia and identification of differentially abundant proteins

Fasting plasma concentration increased by more than twofold in the HHcy group (16.6±1.4 vs. 7.2±0.6 μmol/l). This increase corresponds to the mild HHcy.

Overall, 182 spots on 2D gels were matched in both groups. Automated image analysis detected 46 spots that were differentially abundant in the HHcy group as compared to the control. These spots were analyzed by MALDI-TOF MS/MS. Following Mascot database searching 32 of these spots were successfully identified. Of these, 11 spots were upregulated and 21 downregulated. Identified spots corresponded to 22 different proteins (Fig. 1) because some proteins (ATP synthase subunit α, creatine kinase M-type, aconitate hydratase, and actin) appeared in various spots. These variants possibly resulted from posttranslational modifications of proteins. Table 1 shows the results of identification with one representative of these variants selected according to molecular weight (Mw) and isoelectric point (pI) values close to theoretical values. Based on their cellular location, 5 of the differentially abundant proteins are of mitochondrial origin, 11 are cytoplasmic, 5 are components of myofilaments/cytoskeleton and 1 is nuclear/cytoplasmic. These proteins were found to be involved in various biological processes, including cellular metabolic processes, response to stress, phosphate-containing compound metabolic processes, response to oxidative stress, and muscle contraction.

To verify abundance differences between HHcy and the control group, we performed Western blot analysis with specific antibodies to 8 candidate proteins (α-enolase, β-enolase, myoglobin, isocitrate dehydrogenase, malate dehydrogenase, triosephosphate

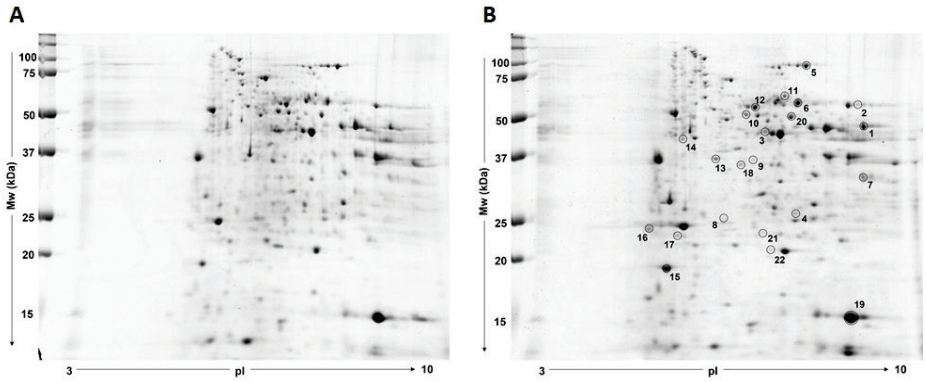

Fig. 1. Representative results of 5 independent experiments for the 2D gel electrophoresis of cardiac proteins isolated from control (**A**) and hyperhomocysteinic rats (**B**). Protein spots that were significantly altered and were successfully identified are marked in circles and manually numbered. Spot numbers correspond to those listed in Tables 1 and 2.

Table 1. Identification of proteins differentially expressed under HHcy

Spot no.	Protein name	UniProt accession no.	Gene ID	Fold change	P value	MS Score	Matched peptides	Sequence coverage (%)
1	Isocitrate dehydrogenase [NADP]	***P56574***	***Idh2***	0.40	0.046	413	20	37
2	ATP synthase subunit α	P15999	Atp5f1a	3.42	0.029	520	24	49
3	Creatine kinase M-type	P00564	Ckm	0.26	0.033	97	7	17
4	Triosephosphate isomerase	P48500	Tpi1	0.38	0.012	370	12	50
5	Aconitate hydratase	Q9ER34	Aco2	0.40	0.0002	611	23	34
6	Succinyl-CoA:3-ketoacid coenzyme A transferase 1	B2GV06	Oxct1	0.49	0.046	269	16	36
7	Glyceraldehyde-3-phosphate dehydrogenase	P04797	Gapdh	0.38	0.018	290	11	43
8	Heat shock protein β-1	P42930	Hspb1	0.36	0.032	151	5	24
9	Aldose reductase	P07943	Akr1b1	0.46	0.044	203	8	22
10	***α-enolase***	P04764	Eno1	0.33	0.001	388	16	50
11	Pyruvate kinase PKM	P11980	Pkm	0.44	0.009	366	17	33
12	Pyruvate dehydrogenase E1 component subunit α	P26284	Pdha1	0.33	0.024	305	16	27
13	L-lactate dehydrogenase B chain	P42123	Ldhb	0.46	0.021	351	14	44
14	Actin, α cardiac muscle 1	P68035	Act1	2.06	0.010	288	11	33
15	Myosin regulatory light chain 2, ventricular/cardiac muscle isoform	P08733	Myl2	3.07	0.001	525	16	95
16	Myosin light chain 3	P16409	Myl3	2.87	0.014	102	4	26
17	Myosin light chain 4	P17209	Myl4	3.02	0.004	108	5	36
18	Malate dehydrogenase, cytoplasmic	O88989	Mdh1	0.49	0.040	283	10	31
19	Myoglobin	Q9QZ76	Mb	2.90	0.002	429	7	53
20	β-enolase	P15429	Eno3	0.43	0.011	280	10	30
21	Glutathione peroxidase 1	P04041	Gpx1	0.48	0.004	130	5	24
22	α-crystallin B chain	P23928	Cryab	0.25	0.037	76	4	18

Spot numbers refer to numbers indicated in Fig. 1. Proteins were identified by 2-DE followed by combined MS and MS/MS analysis.

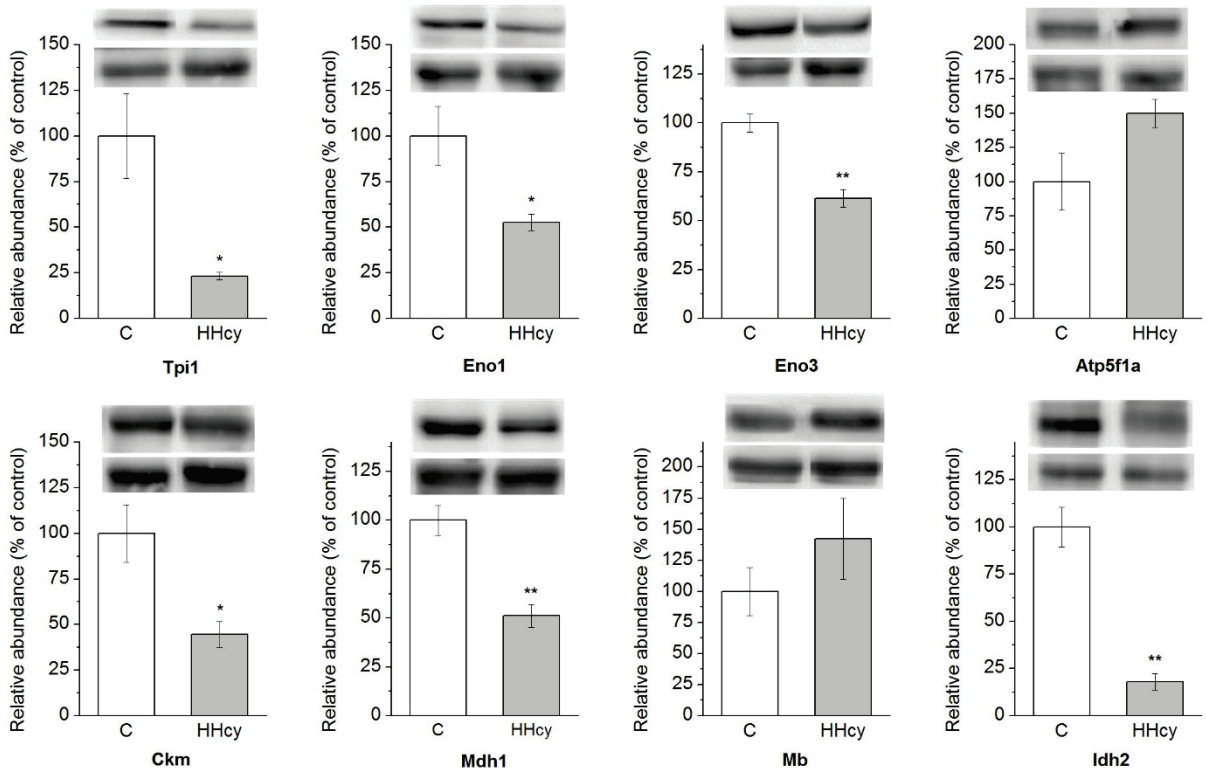

Fig. 2. Effect of HHcy on relative abundances of cardiac proteins as determined by Western blot analysis. Bar graphs represent band volumes given as mean±SEM of 4 experiments. * P<0.05, ** P<0.01; significantly different as compared to control. Representative bands are also shown, the upper left band corresponds to control and the right to HHcy, and the lower bands correspond to β-actin.

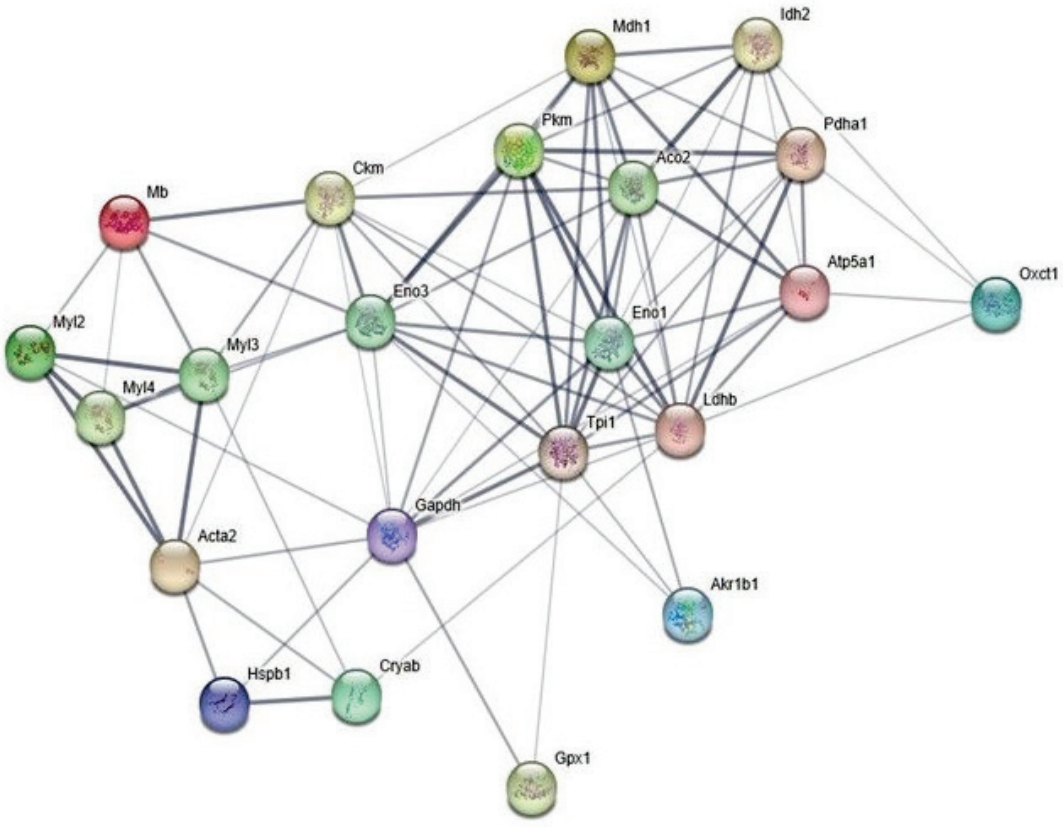

Fig. 3. Protein-protein interactions generated by the STRING software analysis of proteins differentially expressed at HHcy.

Table 2. Functional classification of proteins differentially expressed under HHcy

Spot number	Protein name	Location	Function
1	Isocitrate dehydrogenase [NADP]	Mitochondria	Intermediary metabolism and energy production, $NADP^+$ metabolic process
2	ATP synthase subunit α	Mitochondria	ATP biosynthetic process
3	Creatine kinase M-type	Cytoplasm	Energy transduction
4	Triosephosphate isomerase	Cytoplasm	Glycolysis
5	Aconitate hydratase	Mitochondria	Citric acid cycle
6	Succinyl-CoA:3-ketoacid coenzyme A transferase 1	Mitochondria	Key enzyme for ketone body catabolism
7	Glyceraldehyde-3-phosphate dehydrogenase	Cytoplasm	Glycolysis
8	Heat shock protein β-1	Cytoskeleton, Cytoplasm	Molecular chaperone, stress resistance and actin organization
9	Aldose reductase	Cytoplasm	Reduction of a wide variety of carbonyl-containing compounds to their corresponding alcohols
10	***α-enolase***	Cytoplasm	Glycolysis, plays a part in various processes such as growth control, hypoxia tolerance
11	Pyruvate kinase PKM	Cytoplasm	Glycolysis
12	Pyruvate dehydrogenase E1 component subunit α	Mitochondrial matrix	Conversion of pyruvate to acetyl-CoA and CO_2
13	L-lactate dehydrogenase B chain	Cytoplasm	Interconversion of pyruvate and lactate
14	Actin, α cardiac muscle 1	Actin filament	Cardiac muscle contraction
15	Myosin regulatory light chain 2, ventricular/cardiac muscle isoform	Myosin complex	Cardiac muscle contraction
16	Myosin light chain 3	Myosin complex	Cardiac muscle contraction, regulatory light chain of myosin
17	Myosin light chain 4	Myosin complex	Cardiac muscle contraction, regulatory light chain of myosin
18	Malate dehydrogenase, cytoplasmic	Cytoplasm	Malate-aspartate shuttle
19	Myoglobin		Reserve supply of oxygen, facilitates the movement of oxygen within muscles
20	β-enolase	Cytoplasm	Glycolysis, appears to have a function in striated muscle development and regeneration
21	Glutathione peroxidase 1	Cytoplasm	Cell redox homeostasis, antioxidant
22	α-crystallin B chain	Nucleus, cytoplasm	Chaperone-like activity, prevents aggregation of various proteins under a wide range of stress conditions

isomerase, creatine kinase M and ATP synthase subunit α). Western blot analysis of these proteins confirmed the data obtained by 2D gel electrophoresis with MS analysis (Fig. 2).

Protein-protein interactions of differentially abundant proteins were analyzed using the STRING database. Analysis showed that the network has significantly more interactions than expected for a random set of proteins (Fig. 3). Details of bioinformatic analysis are shown in Table 2.

Antioxidant defense and protein modification

To evaluate the role of oxidative stress in HHcy we determined glutathione levels and total antioxidant capacity as markers of cellular antioxidant defense. As shown in Fig. 4A and B, the total and reduced (GSH) glutathione decreased by 36±7 and 50±8 %, respectively. Since the concentration of oxidized glutathione (GSSG) was unchanged (1.91±0.20 vs. 1.86±0.15 nmol/mg of protein) the GSH/GSSG ratio was also significantly lowered by HHcy. The total antioxidant capacity decreased to 70±2 % ($p<0.001$) as compared to control (Fig. 4C).

To evaluate whether reduced antioxidant defense would result in protein oxidative/nitrative damage protein nitrotyrosines were determined using the ELISA method. As shown in Fig. 4D, the nitrotyrosine concentration in HHcy was 4.5-fold higher when compared to control.

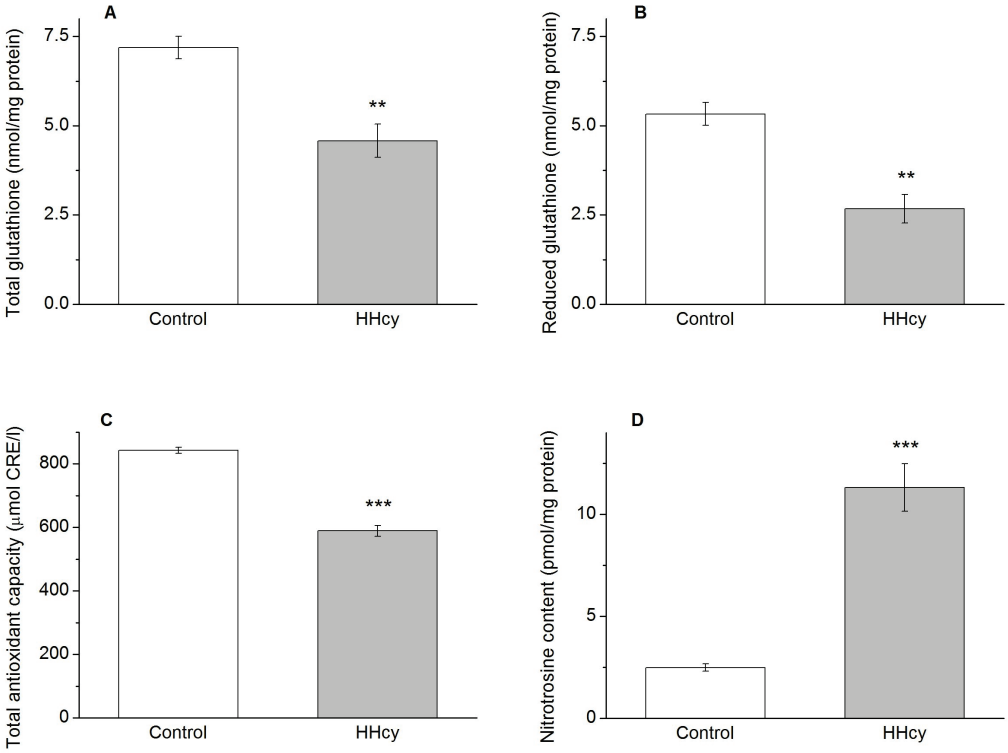

Fig. 4. Effects of HHcy on the total (**A**) and reduced (**B**) glutathione contents, total antioxidant capacity (**C**), and protein tyrosine nitration (**D**) in rat hearts. Values are given as mean ± SEM of 5 experiments. ** $P<0.01$, *** $P<0.001$; significantly different as compared to control.

Discussion

The pathomechanism of HHcy is not yet completely understood. Altered protein expression and cellular oxidative stress have been included among potential contributors to HHcy adverse effects. In this study, we have chosen the model of chronic mild HHcy to investigate the role of these proposed mechanisms in whole-heart homogenates. In our previous studies, we found altered protein expression and unchanged oxidative damage in heart mitochondria and sarcoplasmic reticulum (SR) after this treatment [6,19]. The present study complements previous findings showing that altered are also the expressions of cytoplasmic and myofibrillar proteins. The results of this analysis were confirmed by Western blot studies on selected candidate proteins.

Energy metabolism

Our results suggest that the majority of proteins that were down-regulated under HHcy are involved in the energy-producing pathways. Five proteins participate in glycolysis, triosephosphate isomerase (Tpi), glyceraldehyde-3-phosphate dehydrogenase (Gapdh), α- and β-enolase (Eno1 and Eno3), and pyruvate kinase (Pkm). Tpi catalyzes the reversible interconversion of dihydroxyacetone phosphate and glyceraldehyde-3-phosphate. Gapdh catalyzes the next step, reversible oxidative phosphorylation of glyceraldehyde-3-phosphate into

high-energy phosphate, 1,3-bisphosphoglycerate. Eno1 and Eno3 are α- and β-isoforms of enolase which converts 2-phosphoglycerate into another high-energy compound phosphoenolpyruvate. Finally, Pkm catalyzes the last rate-limiting step in the pathway, the irreversible conversion of phosphoenolpyruvate into pyruvate associated with ATP production. Two other down-regulated proteins are tightly coupled to glycolysis. Ldhb is a subunit B of lactate dehydrogenase that catalyzes the interconversion of pyruvate into lactate. Pdha1 is subunit α of the pyruvate dehydrogenase complex that catalyzes the conversion of pyruvate to acetyl-CoA thereby providing a direct link between glycolysis and the citric acid cycle. Our analysis showed that also one enzyme of the citric acid cycle, aconitase 2, is down-regulated. Aco2, catalyzes the second step of the citric acid cycle, conversion of citrate into isocitrate. ATP synthase is a key enzyme in mitochondrial oxidative phosphorylation that catalyzes the synthesis of ATP from ADP and inorganic phosphate. Our proteomic study shows that in contrast to other proteins involved in energy metabolism, the ATP synthase subunit α is up-regulated in HHcy and this finding was confirmed by Western blot analysis. This finding agrees with our previous observation showing up-regulation of ATP synthase in cardiac mitochondria isolated from HHcy hearts [6] and suggests compensatory mechanisms to prevent diminished ATP production caused by downregulation of glycolytic and other energy-producing enzymes. Oxct1 is mitochondrial succinyl-CoA:3-ketoacid coenzyme A transferase 1 which catalyzes the transfer of coenzyme A from succinyl CoA to acetoacetate. This is the first rate-limiting reaction in ketone body catabolism and its activity was shown to decrease in the heart of diabetic rats [20]. Our result showing down-regulation of Oxct1 suggests the diminished ability of ketone body utilization in HHcy.

From these results, it can be suggested that the catabolic pathways leading to ATP production are significantly deteriorated under HHcy. This is in accordance with the findings of Suematsu et al. [3] who have also reported reduced expression of some of these proteins, namely Gapdh, Pkm and Pdha1, in HHcy.

We also observed the down-regulation of proteins involved in the transfer of high-energy phosphates and reducing equivalents for oxidative phosphorylation in mitochondria. Creatine kinase catalyzes the reversible conversion of ADP and phosphocreatine into ATP and creatine that allows immediate regeneration of ATP. Two CK isoforms, cytosolic and mitochondrial, provide a shuttle of high-energy phosphates between mitochondrial ATP production and cytosolic ATP utilization and phosphocreatine plays a key role in the cellular energy homeostasis. Data on cardiac CK expression under HHcy are not available, loss of CK activity during chronic HHcy was shown in rat skeletal muscle [22] and brain [23]. Cytosolic malate dehydrogenase, Mdh1, catalyzes interconversion between malate and oxaloacetate. Together with mitochondrial Mdh plays an essential role in the malate-aspartate shuttle to transfer reducing equivalents between cytosol and mitochondrial matrix. Literature data on Mdh1 expression in HHcy are lacking, activities of both cytosolic and mitochondrial isoforms were shown to be unaltered in the heart of hyperhomocysteinic rats [24].

Yet another protein related to energy metabolism significantly altered. We observed up-regulation of myoglobin, a cytosolic O_2-binding protein, that acts not only as a reserve supply of O_2 but also as a regulator of myocardial NO homeostasis [25]. NO is a well-known signaling molecule that regulates numerous processes including mitochondrial respiration, therefore one can hypothesize that elevated Mb levels may, via altered NO levels, contribute to disbalance in myocardial energy metabolism. In contrast to our finding, an earlier report shows that the expression of myoglobin is down-regulated [3].

Overall, these findings suggest that chronic HHcy is associated with complex metabolic alterations in the heart.

Contractile proteins

Cardiac muscle contraction is determined by ATP-driven interactions between myosin heads and thin filaments. The α-actin is a major protein of the thin filaments. Cardiac myosin consists of two myosin heavy chains and four myosin light chains, two of them are essential and two are regulatory chains. In this study, we identified 3 myosin light chain proteins that were up-regulated, Myl2, Myl3, and Myl4. Following phosphorylation, ventricular myosin regulatory light chain 2, Myl2 plays a direct role in cross-bridge cycling and calcium-dependent cardiac muscle contraction [26]. Myl3 and Myl4 are essential light chains of ventricular and atrial myosin, that are critically important for cardiac contractility [27,28]. Mutations in genes coding for these three myosin proteins were associated with cardiac hypertrophy [27,29,30]. Data on the expression of

contractile proteins at HHcy are scarce. In contrast to the up-regulation of ventricular Myl2 observed by us, the smooth muscle isoform of Myl2 was shown to be down-regulated in HHcy [3]. Our findings suggest that the up-regulation of α-actin and key regulatory proteins of myosin might be a compensatory mechanism to adopt to disorders in energy metabolism and ATP production in HHcy.

Stress response, antioxidant defense and oxidative stress

Heat-shock protein β1 (HSPB1) and αB-crystallin are small heat-shock proteins that affect various cellular processes such as stress response, structural integrity, and redox balance [31]. HSPB1, which is also known as HSP27, protects against myocardial infarction [32] and down-regulation of HSPB1 was shown to attenuate the reduced state of glutathione reductase and to decrease the GSH/GSSG ratio in H9c2 myoblast cells via modulation of the Hippo signaling pathway [33]. Our findings of down-regulation of HSPB1 and glutathione peroxidase are consistent with those observed in the hearts of dogs with chronic mild HHcy [3]. In addition, our study has shown that these changes are associated with decreased GSH/GSSG ratio and attenuated total antioxidant capacity. Similar disturbances in cardiac GSH homeostasis were observed in mice heterozygous for targeted disruption of cystathionine β-synthase (*Cbs*$^{+/-}$) that was associated with mild HHcy [34]. Loss of function of αB-crystallin was associated with disintegration of myofibrils and accumulation of toxic protein aggregates in muscle fibers [35]. Similarly, a significant decrease of αB-crystallin in the heart was demonstrated in heat-stressed rats [36].

Idh2 is one of two isoforms of mitochondrial isocitrate dehydrogenase, which is NADP-dependent. It catalyzes the oxidative decarboxylation of isocitrate into 2-oxoglutarate associated with the production of NADPH. Accumulating evidence shows that Idh2 is the major NADPH producer in mitochondria and is crucial for the regeneration of GSH or thioredoxin [37]. Knockdown the expression of the Idh2 gene was shown to disrupt the cellular redox balance and induce apoptosis and hypertrophy in cultured cardiomyocytes [38]. Down-regulation of Idh2 could therefore exacerbate HHcy-induced alterations in cellular homeostasis.

Finally, we have found the down-regulation of aldose reductase. Akr1b1 is cytosolic multifunctional enzyme that reduces carbonyl compounds to corresponding alcohols. Under hyperglycemic conditions, AR catalyzes the rate-limiting step of the polyol pathway, which is an important contributor to oxidative stress and diabetic complications. However, under normoglycemic conditions the polyol pathway is negligible and AR is mainly involved in the detoxification of lipid peroxidation-derived reactive aldehydes, such as 4-hydroxynonenal [39,40]. Therefore, the decreased AR content could contribute to cell dysfunction from HHcy-induced injury.

Our data showing that the down-regulation of heat shock proteins and other proteins involved in stress response is accompanied by diminished antioxidant defense as manifested by a decrease in GSH/GSSG ratio and total antioxidant capacity are consistent with studies on H9c2 cells [33]. However, further research is required to elucidate the molecular mechanism by which oxidative defense is diminished in HHcy. Regardless of the mechanism, an imbalance in the redox state seems to result in elevated oxidative damage as demonstrated by the accumulation of protein nitrotyrosines in the heart. Tyrosine nitration is a marker of $ONOO^-$ an attack on proteins and can lead to structural and functional alterations of targeted proteins. Our results are consistent with *in vitro* studies showing that Hcy induces cell death in H9c2 cardiomyocytes through the generation of $ONOO^-$ as monitored by the formation of nitrotyrosines [41]. Studies of Tyagi`s group [42,43] have shown that Hcy-induced tyrosine nitration of matrix proteins leads to impaired diastolic function and myocyte hypertrophy. Our findings are consistent also with studies of Gosh et al. [34] suggesting the link between disturbance in GSH homeostasis and elevated tyrosine nitration.

It is worthwhile to note that in contrast to the present findings, our previous studies using the same model of HHcy demonstrated a lack of oxidative damage in mitochondria and SR, which were isolated from the heart homogenates. These differences suggest that oxidative damage occurs in other cellular structures such as cytosol or plasma membrane. A large number of studies have investigated the role of oxidative stress in the pathomechanism of HHcy demonstrating contradictory results. Our present findings agree with studies supporting the view that alterations in cellular redox state and oxidative damage contribute to HHcy toxicity.

In conclusion, our proteomic study of whole hearts from hyperhomocysteinic rats identified several differentially expressed proteins, mostly involved in energy metabolism, cardiac muscle contraction, cell stress response and antioxidant defense. Furthermore, our

study supports the hypothesis that oxidative stress is involved in the pathomechanism of HHcy. Although the results of our study suggest that altered protein expression is involved in cellular oxidative stress a direct link between these two mechanisms remains to be established.

Conflict of Interest

There is no conflict of interest.

Acknowledgements

This work was partially supported by grants VEGA 1/0004/19 and VEGA 1/0274/23.

References

1. Cziraki A, Nemeth Z, Szabados S, Nagy T, Szántó M, Nyakas C, Koller A. Morphological and functional remodeling of the ischemic heart correlates with homocysteine levels. J Cardiovasc Dev Dis. 2023;10:122. https://doi.org/10.3390/jcdd10030122
2. Perła-Kaján J, Jakubowski H. Dysregulation of epigenetic mechanisms of gene expression in the pathologies of hyperhomocysteinemia. Int J Mol Sci. 2019;20:3140. https://doi.org/10.3390/ijms20133140
3. Suematsu N, Ojaimi C, Kinugawa S, Wang Z, Xu X, Koller A, Recchia FA et al. Hyperhomocysteinemia alters cardiac substrate metabolism by impairing nitric oxide bioavailability through oxidative stress. Circulation. 2007;115:255-262. https://doi.org/10.1161/CIRCULATIONAHA.106.652693
4. Austin RC, Sood SK, Dorward AM, Singh G, Shaughnessy SG, Pamidi S, Outinen PA et al. Homocysteine-dependent alterations in mitochondrial gene expression, function and structure. Homocysteine and H2O2 act synergistically to enhance mitochondrial damage. J Biol Chem. 1998;273:30808-30817. https://doi.org/10.1074/jbc.273.46.30808
5. Cueto R, Zhang L, Shan HM, Huang X, Li X, Li YF, Lopez J et al. Identification of homocysteine-suppressive mitochondrial ETC complex genes and tissue expression profile - Novel hypothesis establishment. Redox Biol. 2018;17:70-88. https://doi.org/10.1016/j.redox.2018.03.015
6. Timkova V, Tatarkova Z, Lehotsky J, Racay P, Dobrota D, Kaplan P. Effects of mild hyperhomocysteinemia on electron transport chain complexes, oxidative stress, and protein expression in rat cardiac mitochondria. Mol Cell Biochem. 2016;411:261-270. https://doi.org/10.1007/s11010-015-2588-7
7. Ungvari Z, Csiszar A, Edwards JG, Kaminski PM, Wolin MS, Kaley G, Koller A. Increased superoxide production in coronary arteries in hyperhomocysteinemia: role of tumor necrosis factor-alpha, NAD(P)H oxidase, and inducible nitric oxide synthase. Arterioscler Thromb Vasc Biol. 2003;23:418-424. https://doi.org/10.1161/01.ATV.0000061735.85377.40
8. Racek J, Rusnáková H, Trefil L, Siala KK. The influence of folate and antioxidants on homocysteine levels and oxidative stress in patients with hyperlipidemia and hyperhomocysteinemia. Physiol Res. 2005;54:87-95. https://doi.org/10.33549/physiolres.930520
9. Wang X, Cui L, Joseph J, Jiang B, Pimental D, Handy DE, Liao R et al. Homocysteine induces cardiomyocyte dysfunction and apoptosis through p38 MAPK-mediated increase in oxidant stress. J Mol Cell Cardiol. 2012;52:753-760. https://doi.org/10.1016/j.yjmcc.2011.12.009
10. Zivkovic V, Jakovljevic V, Djordjevic D, Vuletic M, Barudzic N, Djuric D. The effects of homocysteine-related compounds on cardiac contractility, coronary flow, and oxidative stress markers in isolated rat heart. Mol Cell Biochem. 2012;370:59-67. https://doi.org/10.1007/s11010-012-1398-4
11. Song S, Kertowidjojo E, Ojaimi C, Martin-Fernandez B, Kandhi S, Wolin M, Hintze TH. Long-term methionine-diet induced mild hyperhomocysteinemia associated cardiac metabolic dysfunction in multiparous rats. Physiol Rep. 2015;3:e12292. https://doi.org/10.14814/phy2.12292
12. Liu YP, Zhou GH, Song X, Wang YH, Zhang F, Chen QQ, Cho KW et al. Emodin protects against homocysteine-induced cardiac dysfunction by inhibiting oxidative stress via MAPK and Akt/eNOS/NO signaling pathways. Eur J Pharmacol. 2023;940:175452. https://doi.org/10.1016/j.ejphar.2022.175452
13. Reiter CD, Teng RJ, Beckman JS. Superoxide reacts with nitric oxide to nitrate tyrosine at physiological pH via peroxynitrite. J Biol Chem. 2000;275:32460-32466. https://doi.org/10.1074/jbc.M910433199

14. Kanski J, Beghring A, Pelling J, Schöneich C. Proteomic identification of 3-nitrotyrosine-containing rat cardiac proteins: effect of biological aging. Am J Physiol Heart Circ Physiol. 2005;288:H371-H381. https://doi.org/10.1152/ajpheart.01030.2003
15. Liu B, Tewari AK, Zhang L, Green-Church KB, Zweier JL, Chen YR, He G. Proteomic analysis of protein tyrosine nitration after ischemia reperfusion injury: mitochondria as the major target. Biochim Biophys Acta. 2009;1794:476-485. https://doi.org/10.1016/j.bbapap.2008.12.008
16. Mujumdar VS, Aru GM, Tyagi SC. Induction of oxidative stress by homocyst(e)ine impairs endothelial function. J Cell Biochem. 2001;82:491-500. https://doi.org/10.1002/jcb.1175
17. Sood HS, Cox MJ, Tyagi SC. Generation of nitrotyrosine precedes activation of metalloproteinase in myocardium of hyperhomocysteinemic rats. Antioxid Redox Signal. 2002;4:799-804. https://doi.org/10.1089/152308602760598954
18. Gomez J, Sanchez-Roman I, Gomez A, Sanchez C, Suarez H, Lopez-Torres M, Barja G. Methionine and homocysteine modulate the rate of ROS generation of isolated mitochondria in vitro. J Bioenerg Biomembr. 2011;43:377-386. https://doi.org/10.1007/s10863-011-9368-1
19. Tatarkova Z, Bencurova M, Lehotsky J, Racay P, Kmetova Sivonova M, Dobrota D, Kaplan P. Effect of hyperhomocysteinemia on rat cardiac sarcoplasmic reticulum. Mol Cell Biochem. 2022;477:1621-1628. https://doi.org/10.1007/s11010-022-04399-z
20. Szklarczyk D, Franceschini A, Wyder S, Forslund K, Heller D, Huerta-Cepas J, Simonovic M et al. STRING v10: protein-protein interaction networks, integrated over the tree of life. Nucleic Acids Res. 2015;43:D447-452. https://doi.org/10.1093/nar/gku1003
21. Grinblat L, Pacheco Bolaños LF, Stoppani AO. Decreased rate of ketone-body oxidation and decreased activity of d-3-hydroxybutyrate dehydrogenase and succinyl-CoA:3-oxo-acid CoA-transferase in heart mitochondria of diabetic rats. Biochem J. 1986;240: 49-56. https://doi.org/10.1042/bj2400049
22. Kolling J, Scherer EB, Siebert C, Hansen F, Torres FV, Scaini G, Ferreira G et al. Homocysteine induces energy imbalance in rat skeletal muscle: is creatine a protector? Cell Biochem Funct. 2013;31:575-584. https://doi.org/10.1002/cbf.2938
23. Kolling J, Longoni A, Siebert C, Dos Santos TM, Marques EP, Carletti J, Pereira LO et al. Severe hyperhomocysteinemia decreases creatine kinase activity and causes memory impairment: neuroprotective role of creatine. Neurotox Res. 2017;32:585-593. https://doi.org/10.1007/s12640-017-9767-0
24. Todorovic D, Stojanovic M, Medic A, Gopcevic K, Mutavdzin S, Stankovic S, Djuric D. Four weeks of aerobic training affects cardiac tissue matrix metalloproteinase, lactate dehydrogenase and malate dehydrogenase enzymes activities, and hepatorenal biomarkers in experimental hyperhomocysteinemia in rats. Int J Mol Sci. 2021;22:6792. https://doi.org/10.3390/ijms22136792
25. Hendgen-Cotta UB, Kelm M, Rassaf T. Myoglobin functions in the heart. Free Radic Biol Med. 2014;73:252-259. https://doi.org/10.1016/j.freeradbiomed.2014.05.005
26. Sheikh F, Lyon RC, Chen J. Functions of myosin light chain-2 (MYL2) in cardiac muscle and disease. Gene. 2015;569:14-20. https://doi.org/10.1016/j.gene.2015.06.027
27. Hernandez OM, Jones M, Guzman G, Szczesna-Cordary D. Myosin essential light chain in health and disease. Am J Physiol Heart Circ Physiol. 2007;292:H1643-H1654. https://doi.org/10.1152/ajpheart.00931.2006
28. Sitbon YH, Yadav S, Kazmierczak K, Szczesna-Cordary D. Insights into myosin regulatory and essential light chains: a focus on their roles in cardiac and skeletal muscle function, development and disease. J Muscle Res Cell Motil. 2020;41:313-327. https://doi.org/10.1007/s10974-019-09517-x
29. Melas M, Beltsios ET, Adamou A, Koumarelas K, McBride KL. Molecular diagnosis of hypertrophic cardiomyopathy (HCM): in the heart of cardiac disease. J Clin Med. 2022;12:225. https://doi.org/10.3390/jcm12010225
30. Markandran K, Poh JW, Ferenczi MA, Cheung C. Regulatory light chains in cardiac development and disease. Int J Mol Sci. 2021;22:4351. https://doi.org/10.3390/ijms22094351
31. Christians ES, Ishiwata T, Benjamin IJ. Small heat shock proteins in redox metabolism: implications for cardiovascular diseases. Int J Biochem Cell Biol. 2012;44:1632-1645. https://doi.org/10.1016/j.biocel.2012.06.006

32. Efthymiou CA, Mocanu MM, de Belleroche J, Wells DJ, Latchmann DS, Yellon DM. Heat shock protein 27 protects the heart against myocardial infarction. Basic Res Cardiol. 2004;99:392-394. https://doi.org/10.1007/s00395-004-0483-6
33. Liu X, Liu K, Li C, Cai J, Huang L, Chen H, Wang H et al. Heat-shock protein B1 upholds the cytoplasm reduced state to inhibit activation of the Hippo pathway in H9c2 cells. J Cell Physiol. 2019;234:5117-5133. https://doi.org/10.1002/jcp.27322
34. Ghosh S, Sulistyoningrum DC, Glier MB, Verchere CB, Devlin AM. Altered glutathione homeostasis in heart augments cardiac lipotoxicity associated with diet-induced obesity in mice. J Biol Chem. 2011;286:42483-42493. https://doi.org/10.1074/jbc.M111.304592
35. Dimauro I, Antonioni A, Mercatelli N, Caporossi D. The role of αB-crystallin in skeletal and cardiac muscle tissues. Cell Stress Chaperones. 2018;23:491-505. https://doi.org/10.1007/s12192-017-0866-x
36. Tang S, Chen H, Cheng Y, Nasir MA, Kemper N, Bao E. Expression profiles of heat shock protein 27 and αB-crystallin and their effects on heat-stressed rat myocardial cells in vitro and in vivo. Mol Med Rep. 2016;13:1633-1638. https://doi.org/10.3892/mmr.2015.4693
37. Jo SH, Son MK, Koh HJ, Lee SM, Song IH, Kim YO, Lee YS et al. Control of mitochondrial redox balance and cellular defense against oxidative damage by mitochondrial NADP+-dependent isocitrate dehydrogenase. J Biol Chem. 2001;276:16168-16176. https://doi.org/10.1074/jbc.M010120200
38. Lee JH, Park JW. Attenuated mitochondrial NADP+-dependent isocitrate dehydrogenase activity induces apoptosis and hypertrophy of H9c2 cardiomyocytes. Biochimie. 2014;99:110-118. https://doi.org/10.1016/j.biochi.2013.11.016
39. Liu KX, Li C, Li YS, Yuan BL, Xu M, Xia Z, Huang WQ. Proteomic analysis of intestinal ischemia/reperfusion injury and ischemic preconditioning in rats reveals the protective role of aldose reductase. Proteomics. 2010;10:4463-4475. https://doi.org/10.1002/pmic.201000078
40. Baba SP, Zhang D, Singh M, Dassanayaka S, Xie Z, Jagatheesan G, Zhao J et al. Deficiency of aldose reductase exacerbates early pressure overload-induced cardiac dysfunction and autophagy in mice. J Mol Cell Cardiol. 2018;118:183-192. https://doi.org/10.1016/j.yjmcc.2018.04.002
41. Levrand S, Pacher P, Pesse B, Rolli J, Feihl F, Waeber B, Liaudet L. Homocysteine induces cell death in H9C2 cardiomyocytes through the generation of peroxynitrite. Biochem Biophys Res Commun. 2007;359:445-450. https://doi.org/10.1016/j.bbrc.2007.05.147
42. Sood HS, Cox MJ, Tyagi SC. Generation of nitrotyrosine precedes activation of metalloproteinase in myocardium of hyperhomocysteinemic rats. Antioxid Redox Signal. 2002;4:799-804. https://doi.org/10.1089/152308602760598954
43. Kundu S, Kumar M, Sen U, Mishra PK, Tyagi N, Metreveli N, Lominadze D et al. Nitrotyrosinylation, remodeling and endothelial-myocyte uncoupling in iNOS, cystathionine beta synthase (CBS) knockouts and iNOS/CBS double knockout mice. J Cell Biochem. 2009;106:119-126. https://doi.org/10.1002/jcb.21982